Uniform Ray Description for PO Scattering from Reconfigurable Intelligent Surfaces

E. M. Vitucci[(1)], N. Cenni[(1)], V. Degli-Esposti[(1)], and M. Albani[(2)]
(1) DEI, University of Bologna - Viale Risorgimento, 2, 40126 Bologna, Italy
(2) Department of Information Engineering and Mathematics, University of Siena, Italy

Abstract

An asymptotic approximation of the Physical Optics (PO) integral to compute efficiently the field re-radiated by a metasurface is proposed and discussed. The PO scattered field, including diffraction, is approximated for reflective and transmissive surfaces and cast in a Uniform Theory of Diffraction ray format. A preliminary validation confirms the validity of the approach.

1. Introduction

Reconfigurable Intelligent Surface (RIS) technology has attracted great interest in the last years as an enabling technology for Smart Radio Environments and advanced antenna techniques [1,2]. RIS technology includes a wide range of technical solutions encompassing reflect-array technology with half-wavelength unit cell spacing, as well as metasurface technology making use of electrically small meta-atoms of various shapes and characteristics. In order to perform realistic link-level or system-level simulations of RIS-assisted wireless networks, simple, efficient and yet electromagnetically consistent models for near- and far-field scattering from finite-size RIS are necessary. Unfortunately, most models currently available are either rigorous but complex microscopic models (e.g. based on electromagnetic simulation or on microwave network theory), that require a detailed description of the RIS microstructure, or communication-oriented models conceived for reflect-array realizations where each RIS element can adjust phase and amplitude of its reradiated wave based on the signal received by itself and/or by other array elements according to a "scattering matrix", that is conceived to be optimized for maximum performance [3-5]. Although scattering matrix models are efficient and can account for coupling and non-local effects, they are not very suitable to model metasurface technology realizations, including their multiple parasitic reradiation modes or diffuse scattering effects.
Recently, a general macroscopic model that overlooks the RIS microscopic structure to directly address the wave transformation it realizes through a "spatial modulation coefficient" has been proposed [6], [7]. The model can be applied to metasurfaces as well as to reflectarray-based RIS and accounts for multiple reradiation modes and diffuse scattering. The version of the model described in [6] follows a Huygens-based approach, while in [7] a fully ray-based version of the model is proposed. The latter is based Geometrical Optics (GO) and its extension to diffraction, i.e. the Uniform Theory of Diffraction (UTD), and is more computationally efficient and suitable for integration in forward ray-tracing prediction tools. Such model is however limited to reflective RIS and neglects some phenomena that can be important to predict the scattered field by a finite-size RIS, such as vertex diffraction. A possible way to extend model [7], based on the asymptotic approximation of the PO solution to derive UTD-like diffraction coefficients, is described in the present paper.

2. Proposed extensions of the ray model and discussion

Following the same approach as in [6],[7] we extend the macroscopic ray model to the case of transmissive-RIS (transmissive metasurfaces and transmitarrays), or, more in general, to a RIS which reradiates both in the backward and in the forward (transmission) half-space. In order to do that, we model the RIS as an impedance sheet with different characteristics at the 2 sides: in particular, the RIS has different spatial phase-modulation profiles χ+ and χ- on the sides $\hat{\mathbf{n}}$ and -$\hat{\mathbf{n}}$, respectively, where the normal $\hat{\mathbf{n}}$ to the surface is oriented toward the backward (reflection) half-space. Moreover, we can take into account large scale variations (e.g. non-local effects) and polarization transformations through dyadic amplitude modulation coefficients $\mathbf{\Gamma}_0$ and $\mathbf{T}_0$.
Overall, these effects are considered through the following "spatial modulation" coefficients $\mathbf{\Gamma}$ and $\mathbf{T}$, that accounts for reradiation in the backward and forward half-space, respectively:

$$\begin{cases} \underline{\mathbf{\Gamma}}(\mathbf{r}') = \underline{\mathbf{\Gamma}}_0(\mathbf{r}')\, e^{j\chi^+(\mathbf{r}')} & \mathbf{r}\cdot\hat{\mathbf{n}} > 0 \\ \underline{\mathbf{T}}(\mathbf{r}') = \underline{\mathbf{T}}_0(\mathbf{r}')\, e^{j\chi^-(\mathbf{r}')} & \mathbf{r}\cdot\hat{\mathbf{n}} < 0 \end{cases} \tag{1}$$

where $\mathbf{r}'$ is the position vector of the generic "tile" of the RIS surface, while $\mathbf{r}$ is the position vector of the generic observation point P.

The overall reradiated field by a finite-size RIS, according to the Physical Optics (PO) approach, can be expressed by means of the following radiation integral

$$\mathbf{E}^s(\mathbf{r}) = \frac{jk}{4\pi}\iint_S \hat{\mathbf{R}}\times\left[\mathbf{M}(\mathbf{r}') + \hat{\mathbf{R}}\times\eta\mathbf{J}(\mathbf{r}')\right]\frac{e^{-jkR}}{R}\,dS \tag{2}$$

with $\mathbf{R} = R\hat{\mathbf{R}} = \mathbf{r} - \mathbf{r}'$

Where $\mathbf{J}$ and $\mathbf{M}$ are electric and magnetic currents, respectively, that are computed in the following way, according to the equivalence theorem:

$$
\begin{aligned}
\mathbf{M}(\mathbf{r}) &= \left[\mathbf{E}_0^i e^{-jk\hat{\mathbf{s}}^i\cdot\mathbf{r}} + \underline{\boldsymbol{\Gamma}}\cdot\mathbf{E}_0^i e^{-jk\hat{\mathbf{s}}^i\cdot\mathbf{r}} - \underline{\mathbf{T}}\cdot\mathbf{E}_0^i e^{-jk\hat{\mathbf{s}}^i\cdot\mathbf{r}}\right]\times\hat{\mathbf{n}} \\
\mathbf{J}(\mathbf{r}) &= \frac{\hat{\mathbf{n}}}{\eta}\times\left[\hat{\mathbf{s}}^i\times\mathbf{E}_0^i e^{-jk\hat{\mathbf{s}}^i\cdot\mathbf{r}} + \hat{\mathbf{s}}^r\times\underline{\boldsymbol{\Gamma}}\cdot\mathbf{E}_0^i e^{-jk\hat{\mathbf{s}}^i\cdot\mathbf{r}} - \hat{\mathbf{s}}^t\times\underline{\mathbf{T}}\cdot\mathbf{E}_0^i e^{-jk\hat{\mathbf{s}}^i\cdot\mathbf{r}}\right]
\end{aligned}
\tag{3}
$$

where $\hat{\mathbf{s}}^i$ is the direction of incidence and $\hat{\mathbf{s}}^r$, $\hat{\mathbf{s}}^t$ are the directions of anomalous reflection and anomalous transmission, respectively, that can be expressed as [7]

$$
\begin{cases}
\hat{\mathbf{s}}^r = \left(\underline{\mathbf{1}}-\hat{\mathbf{n}}\hat{\mathbf{n}}\right)\cdot\hat{\mathbf{s}}^i - \frac{1}{k}\nabla\chi^+ + \sqrt{1-\left|\left(\underline{\mathbf{1}}-\hat{\mathbf{n}}\hat{\mathbf{n}}\right)\cdot\hat{\mathbf{s}}^i - \frac{1}{k}\nabla\chi^+\right|^2}\;\hat{\mathbf{n}} \\
\hat{\mathbf{s}}^t = \left(\underline{\mathbf{1}}-\hat{\mathbf{n}}\hat{\mathbf{n}}\right)\cdot\hat{\mathbf{s}}^i - \frac{1}{k}\nabla\chi^- - \sqrt{1-\left|\left(\underline{\mathbf{1}}-\hat{\mathbf{n}}\hat{\mathbf{n}}\right)\cdot\hat{\mathbf{s}}^i - \frac{1}{k}\nabla\chi^-\right|^2}\;\hat{\mathbf{n}}
\end{cases}
\tag{4}
$$

By substituting (1) in (2) and (3), the radiation integral can then be reduced to the following canonic form [8]:

$$
\begin{aligned}
\mathbf{E}^s(\mathbf{r}) = \frac{jk}{4\pi} & \underbrace{\iint_S \underline{\mathbf{G}}^i\cdot\mathbf{E}_0^i\,\frac{e^{-jk\left(\hat{\mathbf{s}}^i\cdot\mathbf{r}'+R\right)}}{R}\,dS}_{\mathbf{A}} + \\
& + \underbrace{\iint_S \underline{\mathbf{G}}^r\cdot\underline{\boldsymbol{\Gamma}}_0\cdot\mathbf{E}_0^i\,\frac{e^{j\left[\chi^+-k\left(\hat{\mathbf{s}}^i\cdot\mathbf{r}'+R\right)\right]}}{R}\,dS}_{\mathbf{B}} + \\
& + \underbrace{\left(-\iint_S \underline{\mathbf{G}}^t\cdot\underline{\mathbf{T}}_0\cdot\mathbf{E}_0^i\,\frac{e^{j\left[\chi^--k\left(\hat{\mathbf{s}}^i\cdot\mathbf{r}'+R\right)\right]}}{R}\,dS\right)}_{\mathbf{C}}
\end{aligned}
\tag{5}
$$

while the dyadic coefficients $\underline{\mathbf{G}}^i$, $\underline{\mathbf{G}}^r$, $\underline{\mathbf{G}}^t$ are computed as [8]:

$$
\underline{\mathbf{G}}^a = \left(\hat{\mathbf{R}}\cdot\hat{\mathbf{n}}\right)\underline{\mathbf{1}} - \hat{\mathbf{n}}\hat{\mathbf{R}} + \left(\underline{\mathbf{1}}-\hat{\mathbf{R}}\hat{\mathbf{R}}\right)\cdot\left[\left(\hat{\mathbf{s}}^a\cdot\hat{\mathbf{n}}\right)\underline{\mathbf{1}} - \hat{\mathbf{s}}^a\hat{\mathbf{n}}\right] \qquad a=i,r,t
\tag{6}
$$

However, the expression (5) is different from the one derived in [8] for a regular surface. In fact, in the case of a RIS modulated through the coefficients in (1) the radiation integral (5) is split into 3 parts (**A**, **B**, **C**): this happens because, differently from [8], it is not possible to take a common phase term for incident, reflected and transmitted field, due to the phase profiles χ+ and χ- applied to reflected/transmitted fields on each element of the RIS surface.

Following the same approach as in [8], the terms **A**, **B**, **C** in (5) can be asymptotically approximated as:

$$
\begin{aligned}
\frac{jk}{4\pi}\mathbf{A} &\simeq -\mathbf{E}^i(P)U^{f,o} + \sum\mathbf{E}^{d,o}(P)U^{e,o} + \sum\mathbf{E}^{v,o}(P) \\
\frac{jk}{4\pi}\mathbf{B} &\simeq \mathbf{E}^r(P)U^{r,a} + \sum\mathbf{E}^{d,ar}(P)U^{e,ar} + \sum\mathbf{E}^{v,ar}(P) \\
\frac{jk}{4\pi}\mathbf{C} &\simeq \mathbf{E}^t(P)U^{f,at} + \sum\mathbf{E}^{d,at}(P)U^{e,at} + \sum\mathbf{E}^{v,at}(P)
\end{aligned}
\tag{7}
$$

The reflected field $\mathbf{E}^r$ and the transmitted field $\mathbf{E}^t$ in (7) are expressed in the following form, according to the GO theory:

$$
\begin{cases}
\mathbf{E}^r(\mathbf{r}) = \underline{\boldsymbol{\Gamma}}(\mathbf{r}')\mathbf{E}^i(\mathbf{r}')\sqrt{\dfrac{\rho_1^r\rho_2^r}{(\rho_1^r+s)(\rho_2^r+s)}}\,e^{-jk_0 s} \\
\mathbf{E}^t(\mathbf{r}) = \underline{\mathbf{T}}(\mathbf{r}')\mathbf{E}^i(\mathbf{r}')\sqrt{\dfrac{\rho_1^t\rho_2^t}{(\rho_1^t+s)(\rho_2^t+s)}}\,e^{-jk_0 s}
\end{cases}
\tag{8}
$$

where s is the local coordinate along the reflected/transmitted ray, and $\rho_1^{r,t}$, $\rho_2^{r,t}$ are the principal curvature radii of the reflected/transmitted wave, which is generally astigmatic, as the phase modulation of the RIS modifies the curvature of the incident wave, as explained in detail in [7]. Here we extend the same approach also to the case of a transmissive RIS. Therefore, the curvature radii of the reflected/transmitted waves are computed as the 2 non-zero eigenvalues of the respective "curvature matrix", in the following way:

$$
\underline{\mathbf{Q}}^{r,t} = \left(\underline{\mathbf{1}} - \frac{\hat{\mathbf{n}}\hat{\mathbf{s}}^{r,t}}{\hat{\mathbf{s}}^{r,t}\cdot\hat{\mathbf{n}}}\right)\left[\underline{\mathbf{Q}}^i - \frac{1}{k_0}\nabla\nabla\chi^{+,-}\right]\left(\underline{\mathbf{1}} - \frac{\hat{\mathbf{s}}^{r,t}\hat{\mathbf{n}}}{\hat{\mathbf{s}}^{r,t}\cdot\hat{\mathbf{n}}}\right)
\tag{9}
$$

where $\underline{\mathbf{Q}}^r,\underline{\mathbf{Q}}^t$ are the curvature matrices of the reflected and transmitted wave, respectively, while $\hat{\mathbf{s}}^r,\hat{\mathbf{s}}^t$ are the directions the reflected and transmitted ray, respectively, computed through (4).

Going back to the asymptotic approximation in (7), it is also evident the presence of separated diffraction contributions that compensate for the abrupt discontinuity of the incident, reflected and transmitted field, respectively, when the observed scattered field goes beyond their domain of existence.

In fact, the function *U* used in (7) is a "step function" which vanishes within the respective ray shadow region, thus bounding the various rays inside their domains of existence. The superscripts *o*, *ar*, *at*, refer to "ordinary", "anomalous reflection" and "anomalous transmission", respectively.

This finding justifies the assumption made in [7], where it was explained through heuristic considerations that diffracted rays that compensate for anomalous reflection belong to an "anomalous Keller's cone" that is different from the "ordinary Keller's cone", made of rays that compensate for incident field. Moreover, we have an Incidence Shadow Boundary (ISB) and an "Anomalous" Reflection Shadow Boundary (ARSB) that belong to the ordinary and to the anomalous Keller's cone, respectively. This is in agreement with the second equation in (7). For the same reason, and in agreement with the third equation in (7), the presence of anomalous transmission gives rise to a further anomalous Keller cone of diffracted rays, and to an Anomalous Transmission Shadow Boundary (ATSB), as depicted in Figure 1.

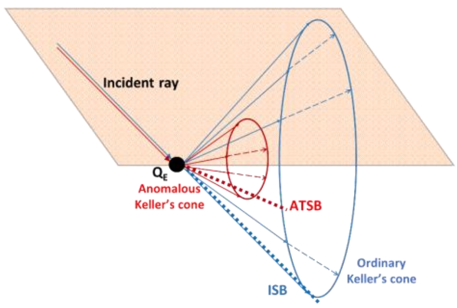

Figure 1. Ordinary Keller's cone and Incidence Shadow Boundary, and corresponding anomalous Keller's cone in the forward half space and Transmission Shadow Boundary.

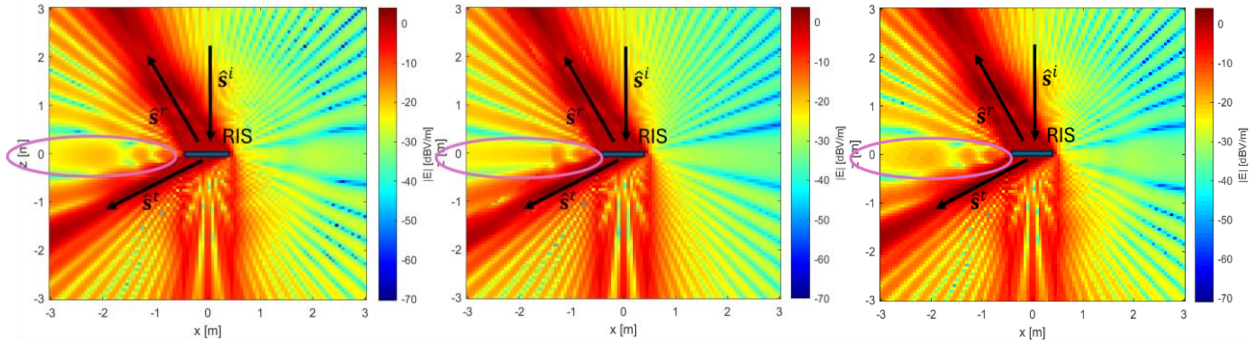

a) Physical Optics integral b) Ray model (no vertex diffraction) c) Ray model with vertex diffraction

Figure 2. Visualization of the reradiated field for a bi-directional (reflective and transmissive) RIS. Normal incident plane wave ($\theta_i = 0$) with $|\mathbf{E_i}| = 1$ V/m. Desired anomalous reflection angle: $\theta_r = 30°$. Desired anomalous refraction angle: $\theta_t = 60°$. The incident power is equally split between the reflection and the forward half-space. a) Numerical solution of the PO integral; b) Ray model based on asymptotic approximation of the PO integral (only edge diffraction is considered); c) Complete ray model (edge and vertex diffraction are considered).

Moreover, from the asymptotic approximation in (7), PO diffraction coefficients can be derived in a straightforward way for both edge and vertex diffraction, following the same procedure as in [8]. The fields diffracted by RIS edges and vertices, respectively, that compensate for the transition of anomalous reflection, are expressed in the following form:

$$\mathbf{E}^{d,ar}(s) = \underline{\mathbf{D}}^{ar} \cdot \mathbf{E}^{i}(Q_E)\sqrt{\frac{\rho^{d,r}}{s(\rho^{d,r}+s)}}\, e^{-jk_0 s} \tag{10}$$

$$\mathbf{E}^{v,ar}(s) = \underline{\mathbf{D}}^{v,ar} \cdot \mathbf{E}^{i}(Q_V)\frac{e^{-jk_0 s}}{s}$$

And the respective diffraction coefficients are:

$$\underline{\mathbf{D}}^{ar} = -\frac{\left[\mathbf{G}^{r}\cdot\mathbf{\Gamma}_0\right]_{Q=Q_E}\cdot e^{-j\frac{\pi}{4}}}{2\sqrt{2\pi k}\,\sin\beta^{d,ar}\left[\left(\hat{\mathbf{s}}^{i}-\hat{\mathbf{s}}^{d,ar}\right)\cdot\hat{\mathbf{t}}-\frac{1}{k}\frac{\partial\chi^{+}}{\partial t}\right]}\Im\left\{X^{E}\right\} \tag{11a}$$

$$\underline{\mathbf{D}}^{v,ar} = \frac{\left|\hat{\mathbf{e}}_1\times\hat{\mathbf{e}}_2\right|\mathbf{G}^{r}\cdot\mathbf{\Gamma}_0(Q_V)}{4j\pi k\left[\left(\hat{\mathbf{s}}^{i}-\hat{\mathbf{s}}^{v}\right)\cdot\hat{\mathbf{e}}_1-\frac{1}{k}\frac{\partial\chi^{+}}{\partial e_1}\right]\left[\left(\hat{\mathbf{s}}^{i}-\hat{\mathbf{s}}^{v}\right)\cdot\hat{\mathbf{e}}_2-\frac{1}{k}\frac{\partial\chi^{+}}{\partial e_2}\right]}T\left\{x_1,x_2,w\right\} \tag{11b}$$

In (11), $\beta^{d,ar}$ is the aperture of the anomalous Keller's cone for reflection, $\hat{\mathbf{s}}^{d,ar}$ is the direction of the diffracted ray that belongs to that cone, and $\hat{\mathbf{t}}$ is a unit vector tangent to the surface, so that $\hat{\mathbf{t}}\times\hat{\mathbf{n}}=\hat{\mathbf{e}}$ with $\hat{\mathbf{e}}$ unit vector along the edge. $\hat{\mathbf{s}}^{v}$ is the direction of the ray diffracted by the vertex toward the observation point, while $\hat{\mathbf{e}}_1, \hat{\mathbf{e}}_2$ are the unit vectors tangent to the 2 adjacent edges forming the vertex. Finally, F and T are the Fresnel transition functions for edge and vertex diffraction, respectively, and their arguments X^E, x_1, x_1, w have the same definition given in [8]. The curvature radius $\rho^{d,r}$ of the diffracted astigmatic wave is computed with the same procedure explained in [7]. Similarly, the fields diffracted by the RIS edges and vertices, that compensate for anomalous transmission, are

$$\mathbf{E}^{d,at}(s) = \underline{\mathbf{D}}^{at} \cdot \mathbf{E}^{i}(Q_E)\sqrt{\frac{\rho^{d,t}}{s(\rho^{d,t}+s)}}\, e^{-jk_0 s} \tag{12}$$

$$\mathbf{E}^{v,at}(s) = \underline{\mathbf{D}}^{v,at} \cdot \mathbf{E}^{i}(Q_V)\frac{e^{-jk_0 s}}{s}$$

and the respective diffraction coefficients are:

$$\underline{\mathbf{D}}^{at} = -\frac{\left[\mathbf{G}^{t}\cdot\mathbf{T}_0\right]_{Q=Q_E}\cdot e^{-j\frac{\pi}{4}}}{2\sqrt{2\pi k}\,\sin\beta^{d,at}\left[\left(\hat{\mathbf{s}}^{i}-\hat{\mathbf{s}}^{d,at}\right)\cdot\hat{\mathbf{t}}-\frac{1}{k}\frac{\partial\chi^{+}}{\partial t}\right]}\Im\left\{X^{E}\right\} \tag{13a}$$

$$\underline{\mathbf{D}}^{v,at} = \frac{\left|\hat{\mathbf{e}}_1\times\hat{\mathbf{e}}_2\right|\mathbf{G}^{t}\cdot\mathbf{T}_0(Q_V)}{4j\pi k\left[\left(\hat{\mathbf{s}}^{i}-\hat{\mathbf{s}}^{v}\right)\cdot\hat{\mathbf{e}}_1-\frac{1}{k}\frac{\partial\chi^{-}}{\partial e_1}\right]\left[\left(\hat{\mathbf{s}}^{i}-\hat{\mathbf{s}}^{v}\right)\cdot\hat{\mathbf{e}}_2-\frac{1}{k}\frac{\partial\chi^{-}}{\partial e_2}\right]}T\left\{x_1,x_2,w\right\} \tag{13b}$$

3. Preliminary results

Preliminary validation results are shown in Fig. 2 and Fig. 3 for a bidirectional reflective/transmissive RIS, configured as an anomalous reflector and anomalous refractor. In both cases, we have a normally incident plane wave, with incident field value $|\mathbf{E_i}| = 1$ V/m. For Fig. 1, the desired (anomalous) reflection and refraction angles are $\theta_r = 30°$ and $\theta_t = 60°$, respectively. For Fig. 2, the desired (anomalous) reflection and refraction angles are $\theta_r = 60°$ and $\theta_t = 30°$, respectively. The incident power is equally split between the reflection and the forward (transmission) half-space, in order to satisfy the overall power balance. In both figures, sub-plots (a) represent the re-radiated field computed through numerical solution of the PO integral in (5). Sub-plots (b) are obtained through the ray model, considering edge diffraction only, where the edge diffraction coefficient is modeled according to (11a) and (13a) for the reflection and transmission half-space, respectively. Finally, in sub-plots (c) also vertex diffraction is added, using the diffraction coefficients of (11b) and (13b). Looking at the results, it can be observed that the ray model, as asymptotic approximation of the PO integral, provides very similar results: however, the computation is about 10 times faster compared to numerical solution of the integral in (5). Moreover, if the vertex diffraction is added, in the ray model, results further improved, especially for reradiation at grazing angles from the RIS (see for example the region inside the magenta ellipses in Figures 2 and 3). In conclusion, the proposed method allows to overcome the limitations of the ray model introduced in [7], by introducing suitable edge and vertex diffraction coefficients for RIS reradiation in both reflection and

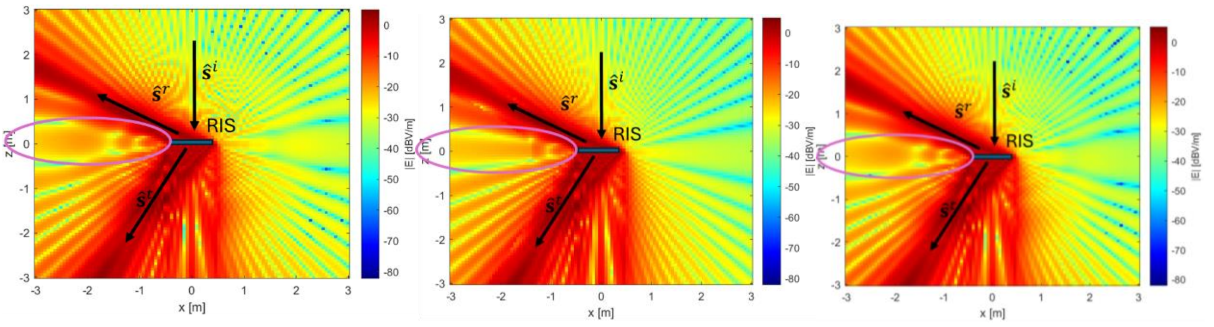

Figure 3. Visualization of the reradiated field for a bi-directional (reflective and transmissive) RIS. Normal incident plane wave ($\theta_i = 0$) with $|\mathbf{E_i}| = 1$ V/m. Desired anomalous reflection angle: $\theta_r = 60°$. Desired anomalous refraction angle: $\theta_t = 30°$. The incident power is equally split between the reflection and the forward half-space. a) Numerical solution of the PO integral; b) Ray model based on asymptotic approximation of the PO integral (only edge diffraction is considered); c) Complete ray model (edge and vertex diffraction are considered).

forward half-space. The accuracy of the proposed approach will be tested in the future in benchmark cases against full-wave simulations and other reference models.

4. Conclusion and future prospects

A framework for computationally efficient prediction of scattering from RISs has been proposed. Starting from the commonly used physical optics (PO) approach, the radiation integral can be asymptotically approximated in order to derive PO UTD-like diffraction coefficients. Then, using the same approach of [7], a complete ray model can be derived, taking into account all the propagation phenomena (anomalous reflection/transmission, edge and vertex diffraction). Preliminary results show that the proposed is very accurate compared to the numerical solution of the PO integral, but with a great advantage in terms of computational efficiency. This approach is suitable for both scattering in the backward (reflection) and forward (transmission) half-space, and is valid for both far-field and near-field radiation regions. In future work, the proposed model will be validated against full-wave numerical simulations, and the PO diffraction coefficients will be compared with the ones heuristically derived in [7].

7. Acknowledgements

This work was supported in part by the European Union under the Italian National Recovery and Resilience Plan (NRRP) of NextGenerationEU, a partnership on “Telecommunications of the Future” (PE0000001 - program “RESTART”). The work is also supported by the Eu Project 6G-SHINE (6G SHort range extreme communication IN Entities), Horizon Europe Programme, Grant No. 101095738, and by the Eu COST Action INTERACT (Intelligence-Enabling Radio Communications for Seamless Inclusive Interactions), Grant CA20120.

References

[1] M. Di Renzo et al., “Smart radio environments empowered by reconfigurable intelligent surfaces: How it works, state of research, and the road ahead,” IEEE J. Sel. Areas Commun., vol.~38, pp. 2450-2525, Nov. 2020.

[2] Q. Wu, S. Zhang, B. Zheng, C. You and R. Zhang, “Intelligent reflecting surface-aided wireless communications: A tutorial,” IEEE Trans. Commun., vol. 69, no. 5, pp. 3313-3351, May~2021.

[3] Q. Wu and R. Zhang, “Beamforming Optimization for Wireless Network Aided by Intelligent Reflecting Surface With Discrete Phase Shifts,” IEEE Trans. Commun., vol. 68, no. 3, pp. 1838-1851, March 2020.

[4] S. Shen, B. Clerckx and R. Murch, “Modeling and Architecture Design of Reconfigurable Intelligent Surfaces Using Scattering Parameter Network Analysis,” IEEE Trans. Wireless Commun., vol. 21, no. 2, pp. 1229-1243, Feb. 2022-

[5] M. Najafi, V. Jamali, R. Schober, H. V. Poor, “Physics-based modeling and scalable optimization of large intelligent reflecting surfaces,” IEEE Trans. Commun., vol. 69, no. 4, pp. 2673-2691, Apr.~2021.

[6] V. Degli-Esposti, E. M. Vitucci, M. Di Renzo and S. A. Tretyakov, "Reradiation and Scattering From a Reconfigurable Intelligent Surface: A General Macroscopic Model," IEEE Trans. Antennas Propag., vol. 70, no. 10, pp. 8691-8706, Oct. 2022.

[7] E. M. Vitucci, M. Albani, S. Kodra, M. Barbiroli and V. Degli-Esposti, "An Efficient Ray-Based Modeling Approach for Scattering from Reconfigurable Intelligent Surfaces," IEEE Trans. Antennas Propag., vol. 72, no. 3, pp. 2673-2685, Mar. 2024.

[8] M. Albani, G. Carluccio, and P.H. Pathak “Uniform Ray Description for the PO Scattering by Vertices in Curved Surface With Curvilinear Edges and Relatively General Boundary Conditions,” IEEE Trans. Antennas Propag., vol. 59, no. 5, pp. 1587-1596, May 2011.